Origin of energetic cosmic rays. I. Galactic diffusion in the energy range 10^{14}-10^{17} eV

1974 J. Phys. A: Math. Nucl. Gen. 7 420

(http://iopscience.iop.org/0301-0015/7/3/013)

J. Phys. A: Math., Nucl. Gen., Vol. 7, No. 3, 1974. Printed in Great Britain.

Origin of energetic cosmic rays
I. Galactic diffusion in the energy range 10^{14}–10^{17} eV

M C Bell, J Kota† and A W Wolfendale

Physics Department, University of Durham, South Road, Durham, UK

Received 5 September 1973, in final form 22 October 1973

Abstract. A brief survey is given of measurements leading to the determination of the energy spectrum of primary cosmic rays in the energy range 10^{14}–10^{17} eV with particular reference to the change of exponent which occurs in the region of 3×10^{15} eV (the spectral 'kink') and an attempt is made to give a quantitative explanation in terms of galactic diffusion.

Reasonable astronomical values for various parameters (cloud sizes, magnetic fields, etc) give some measure of success in accounting for the sharpness of the kink in the energy spectrum, the energy at which it occurs and the magnitude of the change of exponent. Problems arise with the predicted anistropy however and the adopted model breaks down above about 10^{17} eV.

1. Introduction

The present paper is the first of three devoted to attempts to explain the origin of cosmic rays at energies below about 10^{17} eV. In this first paper attention is devoted principally to the energy range 10^{14}–10^{17} eV, in the second work (Karakula *et al* 1974) the range is somewhat similar and in the third paper (Dickinson and Osborne 1974) the energy region examined is lower.

The first two refer primarily to alternative explanations of a rather prominent feature of the primary spectrum: the rapid increase in exponent at an energy of about 3×10^{15} eV. In the present work we start with a detailed examination of the evidence for this change of exponent and a brief summary of important related topics: the magnitude of the anisotropy of arrival directions and the mean mass of the primaries.

At the energies considered here, 10^{14}–10^{17} eV, the intensity of the primary cosmic rays is so low that direct measurements on the particles themselves have not yet proved possible and indirect information has to be used. These indirect studies have comprised an examination of the frequencies of the secondary cascades (extensive air showers: EAS) generated in the atmosphere. At the lower end of the range the measurements are best made at mountain altitudes, because the EAS are so small that the numbers of secondary particles (mainly electrons) reaching sea level is small. At somewhat higher energies, however, the particle numbers are greater and sea level measurements are possible.

As will be shown, and as has been known for some time, the EAS measurements strongly suggest that there is a change of exponent of the primary spectrum, at about 3×10^{15} eV. Expressing the integral spectrum as $AE^{-\gamma}$, the measurements suggest

† On leave from the Central Research Institute of Physics, Budapest, Hungary.

$\gamma \sim 1{\cdot}6$ below 3×10^{15} eV and $\gamma \sim 2{\cdot}2$ at higher energies. Despite earlier evidence for a flattening of the spectrum above about 10^{18} eV it now appears that γ remains virtually constant to the highest energies detected, about 10^{20} eV (see for example the work of Andrews *et al* 1971).

The object of the present paper is to see whether it is possible to give a quantitative explanation of the shape of the primary spectrum and the measured anisotropies in terms of diffusion of cosmic rays in the galaxy. We adopt as our model one in which the cosmic rays of the energies in question are generated within the galaxy by sources whose production spectra have constant exponents and see to what extent an 'astronomically reasonable' distribution of scattering 'centres' and magnetic fields in the galaxy would account for the experimental data. At this stage it is relevant to refer to an alternative approach by Jokipii (1971) using a model in which there is resonant pitch-angle scattering for waves superimposed on a mean field. It appears to us that the problem there lies in the choice of wave spectrum—in the present work we endeavour to use the available astronomical data to give information about the magnetic field irregularities.

Many previous attempts to explain the origin of cosmic rays have, of course, been made (see for example, the reviews by Ginzburg and Syrovatsky 1964, Brecher and Burbidge 1972); the present work differs in that an attempt is made to explain rather specific experimental features in a restricted energy range.

2. Experimental data on the primary cosmic rays

2.1. The primary spectrum of EAS

2.1.1. Method of study. As mentioned in § 1 the experimental data comprise measurements of secondary particles in showers. These measurements take the form of the numbers of particles traversing detectors distributed over a near horizontal surface at ground level, and the data are recorded for each shower whose axis appears to fall in a specified area. From the 'lateral structure function', which is determined from measurements on many showers, the total number of particles in the shower at the recording level is estimated. This is the so-called shower 'size' and the frequency distribution of shower sizes gives the 'size spectrum'. If the full details of the nuclear physical processes occurring in the atmosphere are known, and if the mass of the primary cosmic ray is also known, then the primary energy spectrum can be estimated.

2.1.2. Electron size spectrum. Over the years very many measurements of the electron size spectrum have been made with a variety of detectors and with varying degrees of precision. In the present work we have selected what appear to be the most precise mountain altitude and sea level measurements and these are presented in figure 1(*a*). None of the other measurements, of lower precision, appear to be inconsistent with these results.

Inspection of the electron size spectra shows two features:

(i) There appears to be a transition from a region of virtually constant exponent to another of greater exponent. The change in exponent is about $0{\cdot}55 \pm 0{\cdot}1$ at sea level and about $0{\cdot}75 \pm 0{\cdot}1$ at mountain altitude. (It should be noted, however, that irregularities in spectral slope may have been smeared out although the observation of the quite sharp change in slope suggests that resolution is such as to preclude large irregularities).

(ii) The transitional region is rather short, ie there is a sharp change of slope. A useful quantity, f, can be defined to represent the degree of sharpness, as follows. Draw

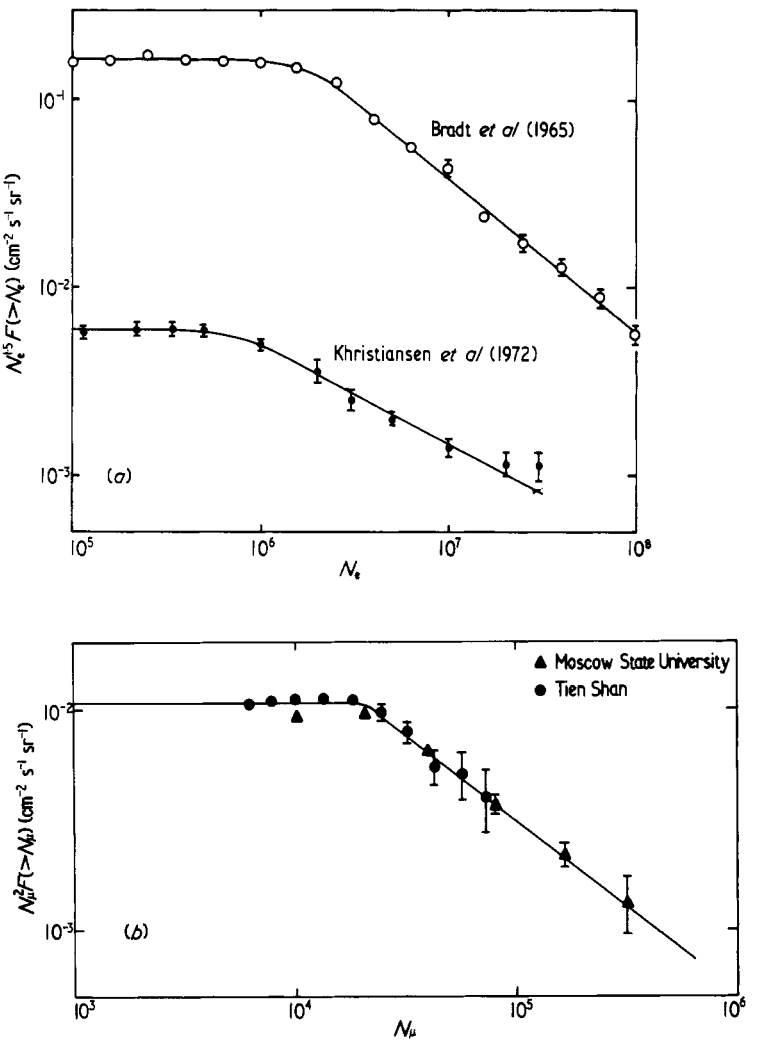

Figure 1. (*a*) The integral size spectrum of EAS at sea level (Khristiansen *et al* 1972) (this unpublished work summarizes the experiments done at Moscow State University and Tian Shan over a number of years) and at a depth of 540 g cm^{-2} (Bradt *et al* 1965). (There are sea level frequencies at larger values of N_e from other experiments, not shown, which confirm the straightness of the line to at least 10^8 particles. (*b*) The integral size spectrum of muons standardized to sea level (Khristiansen *et al* 1972).

best lines through the data points well away from the transition region, let these intersect at a size N_0 and spectral intensity, J_0 ($>N_0$). Now draw a 'smooth' curve through the experimental points and determine the spectral intensity at N_0: $J(>N_0)$. Then $f_i = J(>N_0)/J_0(>N_0)$. Similarly, the factor for differential intensities can be defined as $f_d = j(N_0)/j_0(N_0)$. Inspection of figure 1(*a*) suggests that $f_i \gtrsim 0{\cdot}8$.

2.1.3. Muon size spectrum. Although there are fewer muons than electrons in a shower (μ/e $\sim$ 10%) the fluctuations in muon number for the same primary energy are smaller

(de Beer *et al* 1966) and the data are useful. The most precise data for the energy range in question are probably those of the Moscow group and their results are shown in figure 1(*b*). Again the rapid change of slope is rather marked and it appears that $f_i \gtrsim 0{\cdot}85$.

2.1.4. Conclusions regarding the primary spectrum. The interpretation of the data on the size spectra is that there is very probably a change of exponent of the energy spectrum of the primary particles, from about $\gamma_i \simeq 1{\cdot}6$ between 10^{14} eV and 3×10^{15} eV to $\gamma_i \simeq 2{\cdot}2$ at higher energies (as was mentioned in § 1). It should be remarked however that this conclusion is based to some extent on the assumptions as to the nuclear physics of the processes in the atmosphere and there is just the possibility that these processes differ so greatly from the assumptions as to seriously modify the conclusion. In what follows, we assume that the experimental data do indicate two regions of near constant exponent.

The high value of f_i represents a fact of some interest and importance insofar as many 'noise' factors work to make the transition region for measured electron size greater than the corresponding region for primary energy and thus reduce f_i. These factors are, principally, the effect of fluctuations in longitudinal shower development and sampling errors for the experimentally measured particle densities. The effect of noise on the spectrum is considered in some detail in appendix 1. It is shown there that a differential primary spectrum having a perfectly sharp change of exponent would give $f_i \simeq 0{\cdot}85$ for the measured sea level electron size spectrum; the experimental value of $f_i \gtrsim 0{\cdot}8$ would thus appear to indicate that the primary spectrum does, indeed, have a very sharp change of exponent with, certainly $f_d \gtrsim 0{\cdot}85$ and probably $\gtrsim 0{\cdot}9$.

It is also relevant to point out at this stage that there is some evidence, as yet unsubstantiated, that there may be a region of the primary spectrum between about 2×10^{14} eV and 10^{15} eV where γ_i is smaller than 1·6. Specifically, Wdowczyk and Wolfendale (1973) suggest that $\gamma_i \simeq 1{\cdot}44$. This change is not of great significance in the present work but it has some relevance to the following paper, II.

2.2. The measured anisotropy of cosmic rays

Any divergence from isotropy of the primary cosmic radiation would have immediate relevance to the origin problem. A summary of all the available data has been made recently by Dickinson and Osborne (1974), (paper III). These workers conclude that there is no evidence for a significant anisotropy at any energy; the upper limit (one standard deviation) to the anisotropy from their summary is given later in figure 7.

2.3. The mass spectrum of cosmic rays

Insofar as no direct mass measurements have been made in the energy region in question a definitive answer to the composition question is not possible. What evidence there is, from a variety of indirect experiments, most of which relate to fluctuation in observed quantities, seems to suggest that there is not much change in composition compared with the region below 10^{12} eV/c where direct measurements have been made, ie that protons predominate (see the summaries by Trümper 1970 and Thomson *et al* 1970). In our preferred model, mainly proton primaries are assumed.

3. Diffusion of cosmic rays in the galaxy in the absence of a significant large scale field

3.1. General remarks

As remarked in § 1, the intention is to see to what extent a model involving the diffusion of galactic cosmic rays is able to explain the experimental data on the spectrum and anisotropy.

In what follows, diffusion is first considered in a medium having scattering centres of variable 'power' and then the effect of a superposed uniform field is considered. In each case the characteristics of the interstellar medium expected from astronomical evidence will be assessed and reasonable parameters will be adopted.

It should be remarked at this stage that there have already been suggestions that there should be a change in the primary spectrum at approximately 10^{16} eV due to the presence of scattering in homogeneities of size about 10 pc (eg Goryunov *et al* 1962). In the present work the problem is examined in much more detail.

3.2. Impact parameter method for scattering 'centres'

3.2.1. Uniform clouds. In this idealized treatment it is assumed that there are clouds present in the galaxy which contain magnetic fields. Simplifying assumptions are that the fields are of equal magnitude and that the clouds are spheres of equal diameter. The object at this stage is to calculate the way in which the effective mean free path $\lambda(p)$ will vary with momentum, p.

If the radius of the clouds is R and the field strength H then a characteristic momentum p_0 can be defined such that $p_0c = 300RH$ (with p_0c in eV, R in cm and H in G). Provided $R \ll l$, the mean separation of the spheres along a line of sight, then clearly $\lambda = kl$ for $p \ll p_0$ (where k is a geometrical constant of order unity). For $p \gg p_0$ the solution is well known: $\lambda(p) = kl(p/p_0)^2$ (eg Ginzburg and Syrovatsky 1964). What does not appear to be well known is the form of $\lambda(p)$ for p close to p_0; this is needed if an attempt is to be made to understand the behaviour of the spectral shape in the region of the 'kink'.

When calculating the particle's deflection in a cloud, we adopt a simple two-dimensional model where the clouds are represented by circles with a magnetic field perpendicular to the plane of motion and directed up and down with equal probabilities. In a three-dimensional treatment the particle direction varies with respect to the magnetic field's direction (and so does the effective diameter of the cloud), but the effect of averaging over the various angles on the resulting mean deflection is small.

Consider a particle of momentum p incident as shown in figure 2. The impact parameter is $R \sin\alpha$ and the deflection ϕ is given by $\tan(\phi/2) = R\cos\alpha(R_G + R\sin\alpha)^{-1}$ where R_G is the gyroradius ($= p_0c/(300H)$).

It follows that

$$\cos\phi = 1 - 2p_0^2\cos^2\alpha\,(p^2 + p_0^2 + 2pp_0\sin\alpha)^{-1}.$$

The mean free path is given by $\lambda(p) = l/\psi(p, p_0)$, where $\psi(p, p_0) = \langle 1 - \cos(\phi(p, p_0))\rangle$, the averaging to be carried out over the impact parameters, which are randomly distributed. It follows that

$$\psi(p, p_0) = \tfrac{1}{2}\int_{-1}^{1} 2p_0^2\cos^2\alpha\,(p^2 + p_0^2 + 2pp_0\sin\alpha)^{-1}\,\mathrm{d}(\sin\alpha)$$

$$= \frac{p_0}{p}\left[\frac{1}{2}\left(\frac{p}{p_0} + \frac{p_0}{p}\right) - \frac{1}{4}\left(\frac{p}{p_0} - \frac{p_0}{p}\right)^2 \ln\left|\frac{p+p_0}{p-p_0}\right|\right].$$

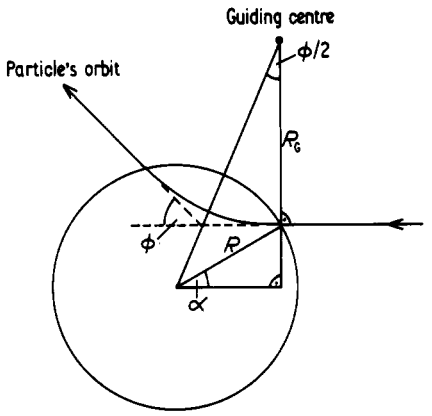

Figure 2. Traversal by a particle of a 'cloud' of magnetic field perpendicular to the diagram (the field may be in the form of a loop without changing the argument appreciably).

Useful values are:

$$\lambda(p, p_0) \begin{cases} = \frac{3}{4}l & \text{for } p \ll p_0 \\ = l & \text{for } p = p_0 \\ = \frac{3}{4}l\left(\frac{p}{p_0}\right)^2 & \text{for } p \gg p_0 \end{cases}$$

(it is noted that the results are as expected for the cases $p \ll p_0$ and $p \gg p_0$).

Of relevance to the cosmic ray case is the fact that under these 'first approximation' conditions the f factor (see § 2.1) is given by $f_d = 0{\cdot}75$. The form $\lambda(p)$ against p is shown in figure 4 (case A) for particular choices of l and p_0. (In fact, in a three-dimensional treatment, f_d will be nearer 0·7.)

3.2.2. Non-uniform clouds. If the clouds are not identical but have a distribution $n(p_0, R)$ (number of clouds eV/c^{-1} per unit radius per unit volume) then the inverse mean free path in the three-dimensional case can be written as

$$\frac{1}{\lambda} = \int_0^\infty \int_0^\infty n(p_0, R)\pi R^2 \psi(p, p_0)\, \mathrm{d}R\, \mathrm{d}p_0 = \int_0^\infty g(p_0)\psi(p, p_0)\, \mathrm{d}p_0$$

where

$$g(p_0) = \int_0^\infty R^2 \pi n(p_0, R)\, \mathrm{d}R,$$

ie the mean number of clouds having the same deflecting power along a line of sight per unit length.

The diffusion coefficient follows as $D = \frac{1}{3}\lambda v$ where v is the particle velocity.

The mean lifetime of a cosmic ray depends of course on the linear dimensions of the system over which the sources and the scattering centres are distributed. If the system is a circular disc of radius b (in fact, the two-dimensional approximation is such that, effectively, we are considering the lifetime in a cylinder) then the mean lifetime of those

particles seen at a point on the axis will be

$$\tau = \frac{b^2}{4D} = \frac{3b^2}{4\lambda v}$$

and if the point of observation is distance x from the axis, the mean lifetime is

$$\tau = \frac{3b^2}{4\lambda v}\left(1 - \frac{x^2}{b^2}\right)$$

for $(x - b)$ greater than several λ.

Application to the case of the solar system and its situation with respect to the spiral arm will now be considered.

3.3. Experimental data on scattering clouds

It is well known that the information on the character of the magnetic field in the galaxy is scanty and in places conflicting. It appears that there are magnetic fields of strength of the order of several microgauss and that these extend over distances of the order of hundreds of parsecs (see, for example, the summary by Roberts 1973). The effect of these large scale fields will be considered later. What concerns us at present is the irregular component of the field which is relevant to much smaller dimensions.

There is a school of thought (eg Parker 1969) which believes that there is a rough balance of energy between the cosmic ray particles and the average magnetic field and that the interaction of the two is associated with the presence of Alfven waves. Insofar as the average energy of the cosmic ray particles as a whole is of the order of several GeV, the Alfven waves will have wavelengths of, typically, 10^{-6} pc and their effect at the 1 pc level will be surely negligible.

There is a variety of information about the irregularities in the interstellar medium, ie about distributions of neutral gas, ionized gas and dust, and there is some evidence for the presence of discrete clouds of material. Of particular relevance is the information on the clouds of gas (HI regions) which contain a significant volume ($\simeq 7\%$, Spitzer 1968), of the gas in the galaxy. Studies of the properties of clouds have been made by many workers (see for example, the work of Spitzer 1968). It is fair to point out that there is uncertainty as to the origin of the clouds (see the discussion by Van de Hulst 1970, and indeed some workers appear to doubt their existence as discrete entities). Of importance in the present work is the frequency distribution of cloud radii and the value of the mean magnetic field in the clouds. (We realize that in fact the clouds will not be completely spherical, but oblateness is not important for this approximate analysis). For a variety of reasons measurements have not been made over an extended region of the local spiral arm but a comprehensive set of high resolution 21 cm data is available from the work of Heiles (1967), Ames and Heiles (1970). These refer to two sheet-like structures of width 10 pc, some 300 and 500 pc from the sun. In these sheets the average hydrogen density is about 1 cm^{-3} compared with about 0·2 cm^{-3} between them. The gas concentrations can be divided into two groups:

(i) *Cloudlets.* Heiles observed 815 cloudlets with n_H (hydrogen density) $\sim 2\ cm^{-3}$ and radii in the range 1–6 pc; and the radii and densities have been given for a representative sample of 45. (It should be noted that lack of resolution limited measurements of radii below 1 pc; there may well be smaller clouds in significant numbers but the

frequency distribution of radii is falling from $R \sim 1{\cdot}5$ pc to smaller sizes so that the frequency of very small cloudlets should not be too large).

(ii) *Clouds*. These volumes have radii in the range 10–40 pc and n_H in the range 2–6 cm^{-3}.

It is these latter clouds which resemble the 'standard' clouds of Spitzer.

The data have been combined together by the present authors; some allowance being made for sampling procedures, to give a measure of the frequency distribution of cloud radii (and, also, of $Rn_H^{2/3}$—see later) over the volume of space subtended by the furthest cloud sheet at the sun. This sheet subtends a solid angle of $40° \times 4°$ and the distance is 500 pc so that the volume is about 2×10^6 pc^3 compared with a sheet volume of only about 2×10^5 pc^3. It is hoped that by taking the diluted density (by a factor of approximately 10) to determine a more reasonable average cloud frequency distribution over the relevant region of space near the sun (the region needed is about 10^7–10^8 pc^3 for particles of momentum 10^{16} eV/c or so). It is appreciated that the procedure adopted is very rough indeed and that gradations of frequency distribution doubtlessly exist in zenith and azimuth which will have an effect on expected anisotropies (see later) but this treatment is the best available at the present time. It must also be borne in mind that the mean separation of the clouds derived from the present survey is uncertain to a factor of 3 or so. The value derived from the analysis is approximately 27 pc along a line of sight, corresponding to $\lambda \simeq 20$ pc.

Turning to the magnetic field measurements, Verschuur (1970) has summarized his own and other Zeeman splitting data for hydrogen clouds in the density range 1–10 cm^{-3} to show that the field strength can be represented by the law $H \simeq 1{\cdot}27 n_H^{2/3}$ for H in μG and n_H in cm^{-3}. This relation is consistent with what would be expected for a contracting cloud containing a frozen-in magnetic field but the data cannot be regarded as proof of this hypothesis; essentially the data show that there are fields in the clouds and that the average over the dimensions of the cloud is as given by the expression—the field may form loops within the cloud and not necessarily be associated with a concentration of an external field.

3.4. Diffusion in the model cloud distribution

The data derived in the previous section can now be used to derive the mean free path as a function of momentum. We assume, as in § 3.2.1, that the field is uniform within a cloud and again proceed by way of the two-dimensional approximation. The final result will be very approximate but would be expected to reproduce the main features of the situation.

The scattering ability of a cloud depends on its area and deflecting power ($p_0 c = 300HR$) and the mean free path is as given in § 3.2.2. We have calculated the p_0 values from the data of Heiles (radii R, and n_H) and Vershuur ($H = 1{\cdot}27 n_H^{2/3}$) and determined the frequency distribution $n(p_0, R)$ and from it the value of

$$g(p_0) = \pi \int R^2 n(p_0, R)\, dR.$$

A plot of $g(p_0)$ against $Rn_H^{2/3}$ is shown in figure 3.

The mean free path then follows from $1/\lambda(p) = \int_0^\infty \psi(p, p_0) g(p_0)\, dp_0$ and the result for $\lambda(p)$ is shown in figure 4. For ease of computation, the function $g(p_0)$ was approximated by two power laws, as shown in figure 3 (broken line). An alternative calculation has also been made using the experimental fact that $Rn_H^{2/3} \simeq 1{\cdot}3 R^{1{\cdot}2}$ ie $R^2 \simeq 0{\cdot}65 (Rn_H^{2/3})^{5/3}$.

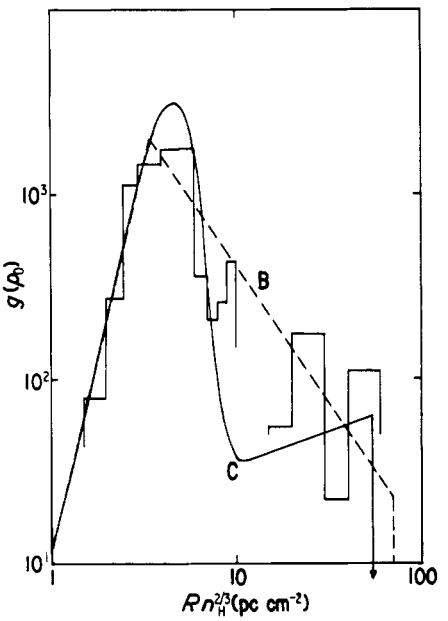

Figure 3. The scattering ability plotted against p_0 from the data of Heiles (1967) and Verschuur (1970) ie $g(p_0)$ against $Rn_H^{2/3}$ ($p_0 \propto Rn_H^{2/3}$). The lines represent alternative fits to the experimental data (see the text).

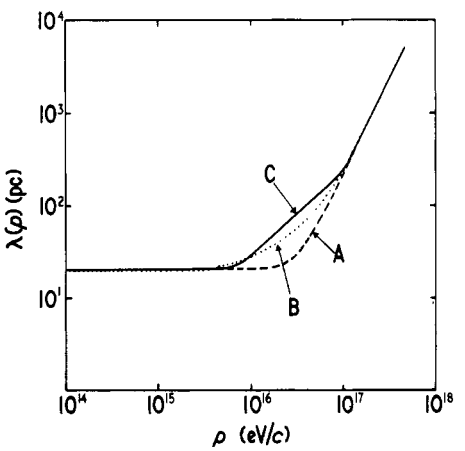

Figure 4. Mean free path plotted against momentum. Case A corresponds to uniform 'spheres', B refers to case B of figure 3 and C corresponds to case C of figure 3.

The operative g function was then found from $f(R)$ alone. In this case $f(R)$ was taken as a near gaussian plus a 'tail', giving rise to the full curve for $g(p_0)$ shown in figure 3. The resulting variations of $\lambda(p)$ for the two forms of $g(p_0)$ are shown in figure 4. Comparison of the two gives an idea of the uncertainty in $\lambda(p)$ arising from alternative treatments of the same experimental data.

The effect of taking a spectrum of cloud diameters (or deflecting powers) is seen to be the production of a region after the kink of momentum over which the slope is

significantly smaller than 2; this reduced slope region extends for rather greater than a decade.

3.5. Comparison of the expected spectral shape with observation

Following the arguments advanced in § 2.3 it is assumed initially that the primary cosmic rays are predominantly protons, and that they are generated uniformly throughout the volume under consideration with a differential spectrum represented by $j(p) = Ap^{-(\gamma+1)}$.

Comparison with experiment can usefully be made by calculating the mean lifetime of the protons from the relation given in § 3.2.2 for the local spiral arm. Here we adopt an idealized arm of radius 300 pc and in the two-dimensional approximation adopted in the present analysis the resulting variation of $\tau(p)$ with p is as shown in figure 5. Calculations have also been made for one special case in three dimensions and the result has been found to be similar. It is not expected that the distortion due to changing to a three-dimensional treatment will be great.

Comparison can be made with the primary spectrum of particles discussed in § 2 expressed in the form $p^{(\gamma+1)}j(p)$ against p—this is equivalent to assuming that the production spectrum of particles follows the law $j(p)\,\mathrm{d}p \propto p^{-(\gamma+1)}\,\mathrm{d}p$ at all momenta, the increase in slope of the measured primary spectrum then coming from the falling lifetime in the spiral arm. The following features are apparent from the comparison:

(i) The position of the kink is within a factor 3 of the experimental value.

(ii) The change of exponent is quite rapid in the case of primary protons, $f_d \simeq 0{\cdot}9$, and not inconsistent with experiment (this for case C in figure 3).

(iii) The predicted change of slope $\Delta\gamma$ is significantly bigger than the measured change above 10^{17} eV.

(iv) Admittedly the estimates of τ are approximate, because of uncertainties in the mean free path, which in turn comes from uncertainties in effective cloud density, but the value below 10^{16} eV of 10^4 yr is much less than the value of approximately 10^6 yr commonly considered to be the case for $E \lesssim 10^{12}$ eV. There could of course be a slow increase of τ with diminishing energy such as to give 10^4 yr at 10^{16} eV/c and about 10^6 yr at 10^{12} eV/c but there appears to be no astronomical evidence in favour of a distribution of scattering centres which would give such a situation.

(v) A big problem arises above 10^{17} eV where the mean free path approaches several hundred parsecs and the so-called 'geometrical limit' is reached. Here the lifetime should tend to be constant (in the absence of any halo effects) and any possibility of agreement with experiment ceases. Furthermore, very large anisotropies of arrival directions should appear.

On balance then, this model, with primary protons, is untenable, except perhaps for energies below about 3×10^{16} eV.

Despite our contention (§ 2.3) that protons are the most likely primaries, calculations have also been made for the situation where the primary composition is 'mixed', ie different elements are present. The particular mixture is taken such that the mass composition is the same at 10^{15} eV/c as that measured directly below 10^9 eV/c (eg by Garcia-Munoz *et al* 1971). Then, because the scattering process depends on rigidity (pc/ze) rather than total momentum, the change of exponent is smaller (this fact appears to have been first pointed out by Peters 1961). These results are also shown in figure 5. Comparison with experiment shows that although the change in slope is more reasonable and f_d is still small, the objections under items (iv) and (v) above remain.

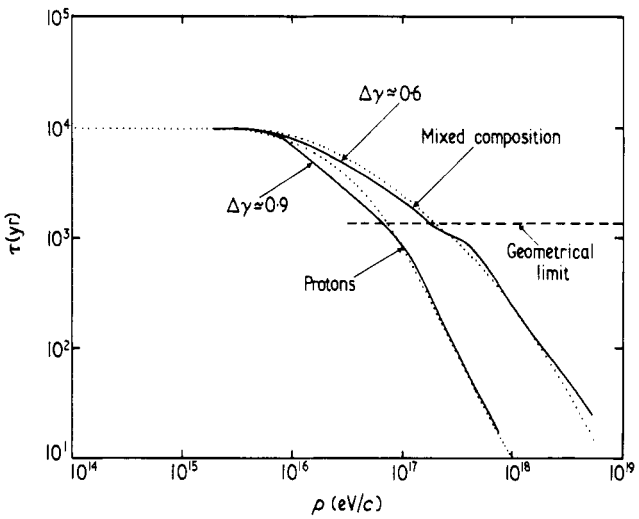

Figure 5. Mean lifetime plotted against momentum for alternative primary mass compositions. No large scale field. Alternative $g(p_0)$ as in figure 3, ie dotted lines, case B; full lines, case C.

In conclusion it appears that the model adopted is, at least, incomplete; its redeeming features are however that the predicted position of the 'kink' is close to the observed one and that quite high f values are possible.

4. Diffusion of cosmic rays in the galaxy in the presence of significant large scale fields

Large scale fields will have the effect of increasing the mean lifetime of the particles and give the possibility of values more in accord with 'observation' (ie about 10^6 yr rather than 10^4 yr).

In the presence of an intercloud field diffusion is not isotropic. It can be described with a diffusion tensor instead of a single diffusion coefficient. The net flow over a surface is given by

$$\boldsymbol{S} = -\frac{\lambda v}{3}\frac{1}{(1+\lambda^2/R_G^2)}\left[\nabla n - \frac{\lambda}{R_G}\boldsymbol{e}\times\nabla n + \left(\frac{\lambda}{R_G}\right)^2 \boldsymbol{e}(\boldsymbol{e}\nabla n)\right]$$

(see for example, Axford 1965) where $\boldsymbol{e}$ is a unit vector pointing in the direction of the intercloud field, λ is the mean free path and R_G is the particle's gyroradius in the intercloud field. The second term does not give outward flow and has no effect on the confinement time (although it contributes to the anisotropy).

The result is different diffusion coefficients along and perpendicular to the field lines:

$$D_{\parallel} = \frac{\lambda v}{3} \qquad D_{\perp} = \frac{\lambda v}{3}\left(1+\frac{\lambda^2}{R_G^2}\right)^{-1}.$$

In fact, the diffusion tensor approximation is only strictly valid for the case where the radii of the scattering 'clouds' are significantly smaller than R_G. The errors introduced into the calculations for the present case are not expected to be large, however. Further errors will arise because of the (unreasonable) assumption of a uniform longitudinal

field. A number of workers have examined the irregularities at the 10–100 pc level (see, for example the work of Osborne *et al* 1973 and Jokipii and Lerche 1969). These irregularities are not expected to have too much effect in the important region below 10^{17} eV/c.

For the containment volume we consider an ellipsoid, elongated along the field lines (parallel to the spiral arm) in which direction its length is $2a$. The perpendicular dimension is $2b$. The diffusion equation yields a mean lifetime τ given by

$$\frac{1}{\tau} = \frac{1}{\tau_{\parallel}} + \frac{1}{\tau_{\perp}}$$

where

$$\tau_{\parallel} = \frac{3a^2}{2\lambda v}\left(1 - \frac{x^2}{a^2} - \frac{\rho^2}{b^2}\right)$$

and

$$\tau_{\perp} = \frac{3b^2}{4\lambda v}\left(1 - \frac{x^2}{a^2} - \frac{\rho^2}{b^2}\right)\left(1 + \frac{\lambda^2}{R_G^2}\right)$$

x and ρ representing the sun's off-centre position along the a and b directions respectively.

The anisotropies follow as:

$$\delta_{\parallel} = \frac{2\lambda x}{a^2}, \qquad \delta_{\perp} = \frac{2\lambda\rho}{b^2}\frac{1}{1+\lambda^2/R_G^2} \qquad \text{and} \qquad \delta_t = \frac{\lambda}{R}\delta_{\perp}$$

where $\delta_{\parallel}$ represents the anisotropy along the field lines and $\delta_{\perp}$ and δ_t represent the anisotropies radial and tangential in a plane perpendicular to the major axis of the arm. These expressions are valid for $x/a, \rho/b \ll 1$.

Values of x and ρ are very uncertain. It is commonly remarked that the sun is about 10 pc below the plane of symmetry (eg Ginzburg 1971) but there is considerable doubt as to the position with respect to the axis of the arm in the plane of the galaxy. Some authors suggest that the sun is on the inside edge of an arm whereas Weaver's diagram indicates a more nearly central position in the interarm link (Weaver 1970). It seems unlikely that x/a and ρ/b are less than 0·1 and this value is taken so as to give a lower limit to the anisotropy in the calculations.

Values of the lifetime calculated using the equations given earlier in this section are shown in figure 6 for various values of the mean intercloud field and for primary protons. The value of $\lambda(p)$ used in the calculations is that designated B in figure 4. Calculations have also been carried out using curve C and the results are similar to those shown, the main difference being a slightly larger value of f_d.

Inspection of figure 6 shows that the mean lifetime below 10^{15} eV/c is now closer to the expected value ($\simeq 10^6$ yr) and with a mean intercloud field of $H_i = 2\,\mu$G the change of slope is quite rapid ($f_d \simeq 0{\cdot}8$) and the magnitude of the change in exponent, $\Delta\gamma \simeq 1{\cdot}0$ to $p = 10^{17}$ eV/c is not too far from observation. This value of $H_i = 2\,\mu$G would not be at variance with the measurements of mean field over distances of the magnitude in question ($\Delta\gamma$ could probably be reduced to the necessary 0·6 by a small admixture of heavy nuclei).

Unfortunately, problems appear in the predicted anisotropy. Figure 7 shows the measured upper limit to δ (from paper III), together with the components derived for

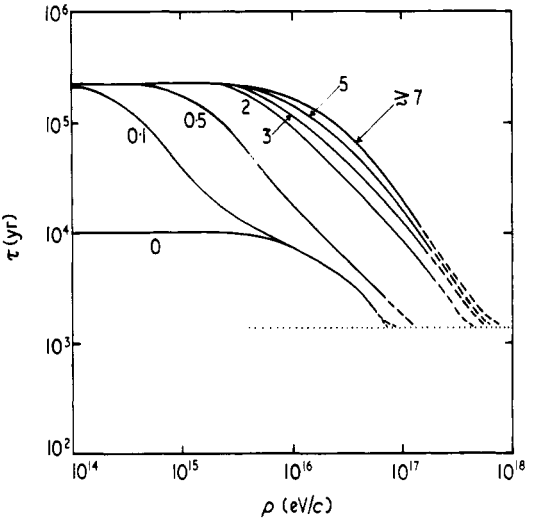

Figure 6. Mean lifetime plotted against momentum for the different values of H_i (the magnitude of the large scale field) shown on the figure (values in μG). $g(p_0)$ is case B of figure 3. The basic physical reason for the increase of τ with H_i is that the field inhibits escape from the surface of the spiral arm.

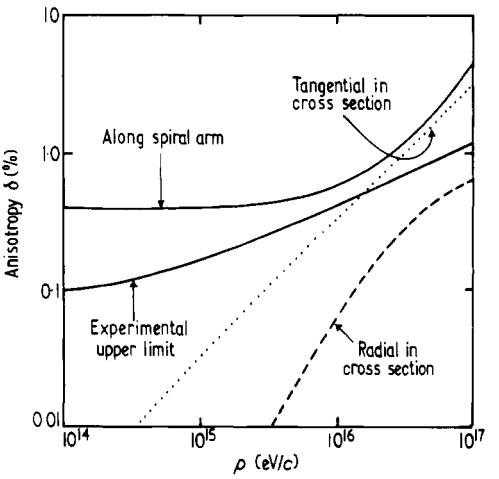

Figure 7. Components of the expected anisotropy vector plotted against momentum. The observable sinusoidal sidereal variation is given by $(I_{max}-I_{min})/(I_{max}+I_{min}) = (\delta_{\parallel}^2+\delta_{\perp}^2+\delta_t^2)^{1/2}$ cos Λ sin χ, (Λ being the declination and χ the anisotropy vector's angle to the earth's axis). With the chosen parameters (10% off-centre in each direction and $H_i = 2\,\mu G$) $\delta_{\parallel}$ dominates at energies below about 5×10^{15} eV, resulting in maximum and minimum intensities along the spiral arm. This corresponds to $(I_{max}-I_{min})/(I_{max}+I_{min}) \simeq 0{\cdot}64\,\delta_{\parallel}$ cos Λ ($\chi \simeq 40°$) and a time of maximum of about RA = 16–17^h (or 4–5^h depending on the off-centre direction). At higher energies the contribution of δ_t becomes comparable with that of $\delta_{\parallel}$. Not only does this affect the measure of the sidereal wave but also manifests itself in a shift of the time of maximum.

the present choice of parameters. At first sight it appears that the model is ruled out because the experimental limit is everywhere below the predicted anisotropies. However, it will be remembered from § 3.3 that the value of λ is uncertain to a factor of 3; if λ were reduced by a factor 3 the longitudinal anisotropy would be reduced accordingly and it might be possible just to remove the inconsistency below about 10^{17} eV/c. A further point of relevance is that the angle between the earth's axis and the spiral arm axis causes an effective reduction in predicted anisotropy. Another advantage of the factor 3 would be to increase the mean lifetime to nearer 10^6 yr. Above 10^{17} eV/c, however, the anisotropy would be surely greater than observed.

5. Conclusions

A model has been constructed in which the primary cosmic rays are mainly protons, from sources distributed within the galaxy in a similar manner to that of stars and gas, and these protons are able to diffuse through the local spiral arm (or rather the interarm link).

The diffusion is governed by interaction with the (magnetized) clouds of hydrogen and the large scale (> 100 pc) galactic magnetic field. Taking data on the gas clouds and cloudlets from the work of Heiles and co-workers, which refer to a particular region of the galaxy, and assuming that it can be used over a much wider region, gives rise to a diffusion coefficient which starts to increase at about the momentum at which the primary cosmic ray spectrum is observed to have a change of slope. This is a rather important success for the model.

With an intercloud field of about 2 μG (an astronomically acceptable value) and a mean free path for collision with clouds a factor of 3 shorter than we would have expected (although still an acceptable value) the mean lifetime of the protons is reasonably close to expectation. Further favourable features are the explanation of the sharp kink in the spectrum and a value for the change of exponent of the energy spectrum not too different from observation.

Problems arise with the predicted anisotropies however. It is necessary to make the rather unreasonable assumption that the solar system is rather close to the effective centre of the scattering system. If the centring assumption is valid then it is probably possible to explain particles up to 10^{17} eV/c as being of galactic origin. At much higher momenta this possibility effectively ceases. The same conclusion has been arrived at from different reasoning by other workers (eg Osborne *et al* 1973). Another way of explaining the low observed anisotropy is of course to assume the existence of a 'halo' having little matter but a significant magnetic field (eg Ginzburg and Syrovatsky 1964) but such an assumption seems rather artificial. A further possibility is a field configuration which does not allow easy escape over distances of the order of a kiloparsec.

Acknowledgments

The Science Research Council is thanked for its support. The authors are grateful to Drs J L Osborne, S Karakula and J Wdowczyk and Mr G J Dickinson for many useful discussions.

Appendix 1. Effect of 'noise' on the EAS electron size spectrum

Let $j(E)$ be a differential primary energy spectrum and consider the case where the spectral form is a simple power law:

$$j(E) \propto E^{-\gamma-1} \qquad \text{and} \qquad J(>E) \propto E^{-\gamma}.$$

Consider a perfect kink in the differential primary spectrum:

$$j(E) = \left(\frac{E}{E_0}\right)^{-\gamma_1-1} \qquad \text{for } E \leqslant E_0$$

$$j(E) = \left(\frac{E}{E_0}\right)^{-\gamma_2-1} \qquad \text{for } E > E_0.$$

Clearly, the integral spectrum will not have a perfectly sharp change of slope (kink) even disregarding the noise which arises from the causes outlined in § 1.

Integrating the differential spectrum gives

$$E_0^{-1}J(>E) = \begin{cases} \dfrac{1}{\gamma_1}\left(\dfrac{E}{E_0}\right)^{-\gamma_1} - \dfrac{1}{\gamma_1} + \dfrac{1}{\gamma_2} & \text{for } E \leqslant E_0 \\ \dfrac{1}{\gamma_2}\left(\dfrac{E}{E_0}\right)^{-\gamma_2} & \text{for } E > E_0. \end{cases}$$

The apparent position of the kink will be the point of intersection of the two asymptotes:

$$E_k = \left(\frac{\gamma_1}{\gamma_2}\right)^{(\gamma_2-\gamma_1)^{-1}} E_0.$$

If $\gamma_1 = 1{\cdot}5$ and $\gamma_2 = 2{\cdot}04$ ('best' values from § 2), $E_k = 0{\cdot}566\,E_0$. Defining the f value in the manner indicated earlier, this choice of constant yields $f_i = 0{\cdot}887$.

This f_i is the ultimate that can be achieved, in the absence of noise, for a perfectly sharp kink in the differential spectrum, $f_d = 1$.

In the practical case, where noise is present we define $\bar{N} = kE$, ie the mean number of electrons is proportional to the primary energy. In fact $\bar{N} \propto E^{\alpha}$ where $\alpha \simeq 1{\cdot}15$ (de Beer *et al* 1966), but writing $\alpha = 1$ has a negligible effect on the object of the calculations: a determination of f_i in the presence of noise.

The calculations of de Beer *et al* (1966) and others, suggest that the resolution can be described roughly by a gaussian distribution on a logarithmic plot:

$$h(N, \bar{N}) = \frac{1}{\sqrt{2\pi\sigma^2}} \exp\left(-\frac{\ln(N/\bar{N})^2}{2\sigma^2}\right).$$

The assumed linearity of $\bar{N}$ and E means that we can consider $j(\bar{N})$ instead of $j(E)$ since they differ only by a constant factor.

The electron size spectrum follows as

$$F(N) = \frac{1}{N}\int_0^{\infty} h(N, \bar{N})\, j(\bar{N})\, \mathrm{d}\bar{N} \qquad \text{and} \qquad F(>N) = \int_N^{\infty} F(N)\, \mathrm{d}N.$$

If σ is constant, independent of E, then $F(>N)$ follows as

$$F(>N) = \int_{-\infty}^{\infty} h(N, \bar{N}) J(>\bar{N})\, \mathrm{d}\ln\bar{N}.$$

For the case of a perfect kink in $j(E)$, as defined earlier, the result is

$$F(N) = \left(\frac{N}{N_0}\right)^{-\gamma_1-1} \exp\left(\frac{\gamma_1^2\sigma^2}{2}\right) \int_{-\infty}^{S_1} \frac{1}{\sqrt{2\pi}} \exp\left(\frac{-x^2}{2}\right) dx$$
$$+ \left(\frac{N}{N_0}\right)^{-\gamma_2-1} \exp\left(\frac{\gamma_2^2\sigma^2}{2}\right) \int_{S_2}^{\infty} \frac{1}{\sqrt{2\pi}} \exp\left(\frac{-x^2}{2}\right) dx,$$

where

$$S_1 = -\frac{1}{\sigma} \ln \frac{N}{N_0} + \gamma_1\sigma$$

and

$$S_2 = -\frac{1}{\sigma} \ln \frac{N}{N_0} + \gamma_2\sigma.$$

The result is that

$$f_d = 1 - \text{erf} \frac{(\gamma_2 - \gamma_1)\sigma}{2\sqrt{2}}.$$

As expected, $f_d \to 1$ as $\sigma \to 0$ and f_d decreases as σ increases.

The effect of various values of σ on the expected size spectrum (differential and integral) is shown in figure 8. For measurements near sea level it seems that $\sigma \simeq 0{\cdot}5$ (de Beer *et al* 1966) and the operative values of f are $f_d = 0{\cdot}90$ and $f_i = 0{\cdot}85$.

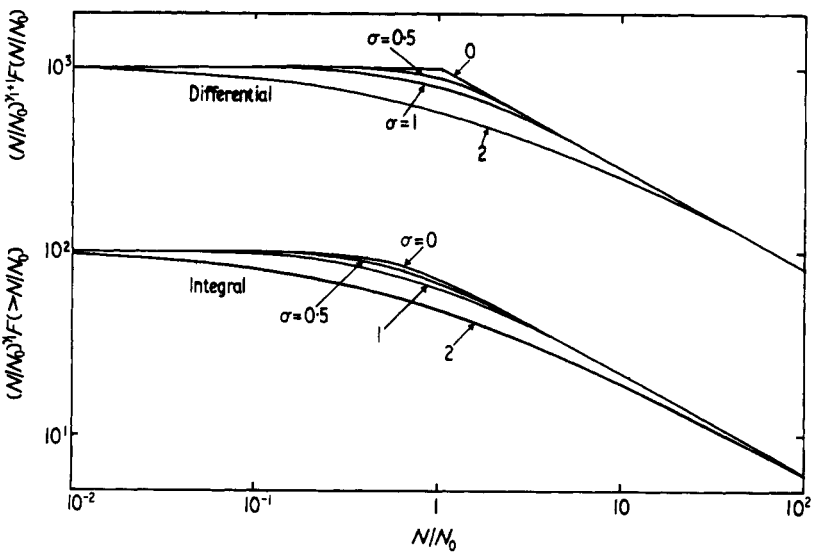

Figure 8. Effect of noise on the size spectrum due to a primary spectrum having a sharp change of exponent (see appendix 1).

References

Ames S and Heiles C 1970 *Astrophys. J.* **160** 59–64

Andrews D *et al* 1971 *Proc. 12th Int. Conf. on Cosmic Rays, Hobart* vol 3 (Hobart: University of Tasmania) pp 995–1000

Axford W I 1965 *Planet. Space Sci.* **13** 115
Bradt H *et al* 1966 *Proc. 9th Int. Conf. on Cosmic Rays, London* vol 2 (London: The Institute of Physics and The Physical Society) pp 715–7
Brecher K and Burbidge G R 1972 *Astrophys. J.* **174** 253–91
de Beer J F, Holyoak B, Wdowczyk J and Wolfendale A W 1966 *Proc. Phys. Soc.* **89** 567–85
Dickinson G and Osborne J L 1974 *J. Phys.* A: *Math., Nucl. Gen.* **7** in the press
Garcia-Munoz M *et al* 1971 *Proc. 12th Int. Conf. on Cosmic Rays, Hobart* vol 1 (Hobart: University of Tasmania) pp 209–14
Ginzburg V L and Syrovatsky S I 1964 *The Origin of Cosmic Rays* (Oxford: Pergamon)
—— 1971 *Proc. 12th Int. Conf. on Cosmic Rays, Hobart* (Hobart: University of Tasmania) Invited and Rapporteur Papers pp 53–71
Goryunov *et al* 1962 *Bull. Acad. Sci. USSR* **46** 684
Heiles C 1967 *Astrophys. J. Suppl.* **15** 97–130
Karakula S, Osborne J L and Wdowczyk J 1974 *J. Phys.* A: *Math., Nucl. Gen.* **7** 437–43
Khristiansen G B *et al* 1972 *Eur. Symp. on Cosmic Rays, Paris*
Jokipii J R 1971 *Proc. 12th Int. Conf. on Cosmic Rays, Hobart* vol 1 (Hobart: University of Tasmania) p 403
Jokipii J R and Lerche I 1969 *Astrophys. J.* 1137–45
Osborne J L, Roberts E and Wolfendale A W 1973 *J. Phys.* A: *Math., Nucl. Gen.* **6** 421–33
Parker E N 1969 *Space Sci. Rev.* **9** 651
Peters B 1961 *Nuovo Cim.* **22** 800–19
Roberts E 1973 *PhD Thesis* University of Durham
Spitzer L 1968 *Diffuse Matter in Space* (New York: Interscience)
Thompson M G *et al* 1970 *Acta Phys. Acad. Sci. Hung.* **29** *Suppl.* 3 615–20
Trümper J 1970 *Proc. 6th Interam. Sem. on Cosmic Rays, La Paz Bolivia* vol 2 (University of San Andreas) p 372
Van de Hulst H C 1970 *IAU Symp.* No 39 (Dordrecht: Reidl) pp 3–17
Verschurr G L 1970 *IAU Symp.* No 39 (Dordrecht: Reidl) pp 150–67
Wdowczyk J and Wolfendale A W 1973 *J Phys.* A: *Math., Nucl. Gen.* **6** L48–51
Weaver H 1970 *IAU Symp.* No 38 (Dordrecht: Reidl) pp 126–239